

Article

Sustainable Synthesis, Antiproliferative and Acetylcholinesterase Inhibition of 1,4- and 1,2-Naphthoquinone Derivatives

Rafaela G. Cabral^{1,2}, Gonalo Viegas¹, Rita Pacheco^{1,2}, Ana Catarina Sousa^{1,2,*}
and Maria Paula Robalo^{1,2,*}

¹ Departamento de Engenharia Qumica, Instituto Superior de Engenharia de Lisboa, Instituto Politcnico de Lisboa, 1959-007 Lisboa, Portugal

² Centro de Qumica Estrutural, Institute of Molecular Sciences, Instituto Superior Tcnico, Universidade de Lisboa, 1049-001 Lisboa, Portugal

* Correspondence: acsousa@deq.isel.ipl.pt (A.C.S.); paula.robalo@isel.pt (M.P.R.)

Abstract: This work describes the design, sustainable synthesis, evaluation of electrochemical and biological properties against HepG2 cell lines, and AChE enzymes of different substituted derivatives of 1,4- and 1,2-naphthoquinones (NQ). A microwave-assisted protocol was optimized with success for the synthesis of the 2-substituted-1,4-NQ series and extended to the 4-substituted-1,2-NQ family, providing an alternative and more sustainable approach to the synthesis of naphthoquinones. The electrochemical properties were studied by cyclic voltammetry, and the redox potentials related to the molecular structural characteristics and the biological properties. Compounds were tested for their potential anti-cancer activity against a hepatocellular carcinoma cell line, HepG2, using MTT assay, and 1,2-NQ derivatives were found to be more active than their 1,4-NQ homologues (3a–f), with the highest cytotoxic potential found for compound 4a ($EC_{50} = 3 \mu\text{M}$). The same trend was found for the inhibitory action against acetylcholinesterase, with 1,2-NQ derivatives showing higher inhibition_{50 μM} than their 1,4-NQ homologues, with 4h being the most potent compound (Inhibition_{50 μM} = 85%). Docking studies were performed for the 1,2-NQ derivatives with the highest inhibitions, showing dual binding interactions with both CAS and PAS sites, while the less active 1,4-NQ derivatives showed interactions with PAS and the mid-gorge region.

Keywords: naphthoquinones; electrochemistry behavior; acetylcholinesterase inhibitory activity; cytotoxic activity; biological activity



check for updates

Citation: Cabral, R.G.; Viegas, G.; Pacheco, R.; Sousa, A.C.; Robalo, M.P. Sustainable Synthesis, Antiproliferative and Acetylcholinesterase Inhibition of 1,4- and 1,2-Naphthoquinone Derivatives. *Molecules* **2023**, *28*, 1232. <https://doi.org/10.3390/molecules28031232>

Academic Editor: Christoffer Bengtsson

Received: 2 January 2023

Revised: 23 January 2023

Accepted: 25 January 2023

Published: 27 January 2023



Copyright: © 2023 by the authors. Licensee MDPI, Basel, Switzerland. This article is an open access article distributed under the terms and conditions of the Creative Commons Attribution (CC BY) license (<https://creativecommons.org/licenses/by/4.0/>).

1. Introduction

Naphthoquinones (NQ) have played a crucial role in the drug discovery process been widely used as important pharmacophores or intermediates for the synthesis of bioactive compounds. These heterocyclic compounds are known to exhibit a diverse range of biological properties, such as antimicrobials, antitumoral, antioxidants, antimalarial, and neuroprotectants, among others [1–3]. Their mechanisms of action are often related to their redox properties, as most have the capacity to accept one or two electrons to generate highly reactive radical species capable of interacting with biological molecules such as DNA, enzymes, and other proteins [4–6]. The electrochemical behavior of these compounds seems to be related to the biological activity and quinone scaffold, with multiple redox functionalities, justifying the continuous interest and efforts to find derivatives with different functionalization and screening for potential biological properties [6–9].

Different types of cancers and several neurodegenerative disorders are often associated with intracellular redox imbalance and consequent oxidative damage [10,11], making NQ appellative compounds for the redox medicine field. Their anticancer activity has attracted widespread attention, and several natural and synthetic naphthoquinones derivatives have been used in cancer therapy, demonstrating to inhibit the proliferation and

induce apoptosis in cancer cells [10–14]. Other works that validate NQ action as selective enzyme inhibitors [15] also showed the potential of using 1,4-NQ and 1,2-NQ derivatives in different therapeutics. Recently, Shin et al. [16] have demonstrated that 1,4-NQ derivatives exhibit neuroprotective effects and may play a key role in the therapeutic strategy against Alzheimer's disease (AD). Moreover, plant extracts rich in natural naphthoquinones, and synthetic naphthoquinone derivatives were reported as acetylcholinesterase inhibitors (AChEIs) [17–22]. The acetylcholinesterase enzyme (AChE, EC 3.1.1.7) plays a major role in the activity of the central and peripheral nervous systems and is one of the main targets of drug therapies for AD [23]. The drugs currently available, such as the AChEIs donepezil, galantamine, and rivastigmine, used in the symptomatic treatment of AD, show non-negligible adverse side effects [24] and the growing importance of neurodegenerative diseases due to the increase in average life expectancy, justifies the search for new alternative leads and the evaluation of the potential of NQ moiety.

The NQ scaffold is undoubtedly important, and the quinone's reactivity can be modulated by introducing atoms or groups into the central naphthoquinone ring, thus encouraging the design of derivatives and the exploration of their electrochemical and biological properties. Amine groups have been reported to play a key role in many bioactive compounds, and literature data have shown that their presence in the quinone backbone tunes its redox properties and induces oxidative stress in cells and DNA alkylation [25]. Aliphatic amine groups are ubiquitously present in a wide range of compounds with proven biological activities [26,27]. Based on these findings, we design new derivatives of 1,4-NQ and 1,2-NQ, where the combination with different amine substituents aims to promote synergistic effects of both moieties.

The NQ derivatives can be prepared by conventional methods with satisfactory yields, although in most cases, with time-consuming protocols and tedious workups. To overcome these restrictions, new, greener synthetic approaches have been explored [28,29]. Microwave-assisted (MA) organic synthesis is considered an important green approach and, nowadays, is widely used in the pharmaceutical industry for the oriented synthesis of target compounds [30,31], allowing for more energy-efficient and cleaner reactions, the choice of green solvents, time-efficient routes, and higher yields. In this context, and as a part of our interest in developing sustainable synthetic protocols, we report herein the synthesis of several 2-substituted-1,4-NQ and 4-substituted-1,2-NQ derivatives by microwave-assisted protocols, the study of their electrochemical behavior and evaluation of their biological potential, namely, as AChE inhibitors and cytotoxic agents in human hepatocarcinoma HepG2 cell line.

2. Results and Discussion

2.1. Synthesis and Characterization

A set of compounds derived from 1,4-NQ and 1,2-NQ were studied (Figure 1) to evaluate the viability of an alternative MA protocol for their synthesis, their biological potential, and the impact of the association of these moieties in the same molecule. Aliphatic amines and substituted anilines with electron donor and acceptor groups have been used as nucleophilic partners since it is known that the electronic nature and position of the substituents in the NQ aromatic rings affect their redox potential and, consequently, the associated biological activities [6].

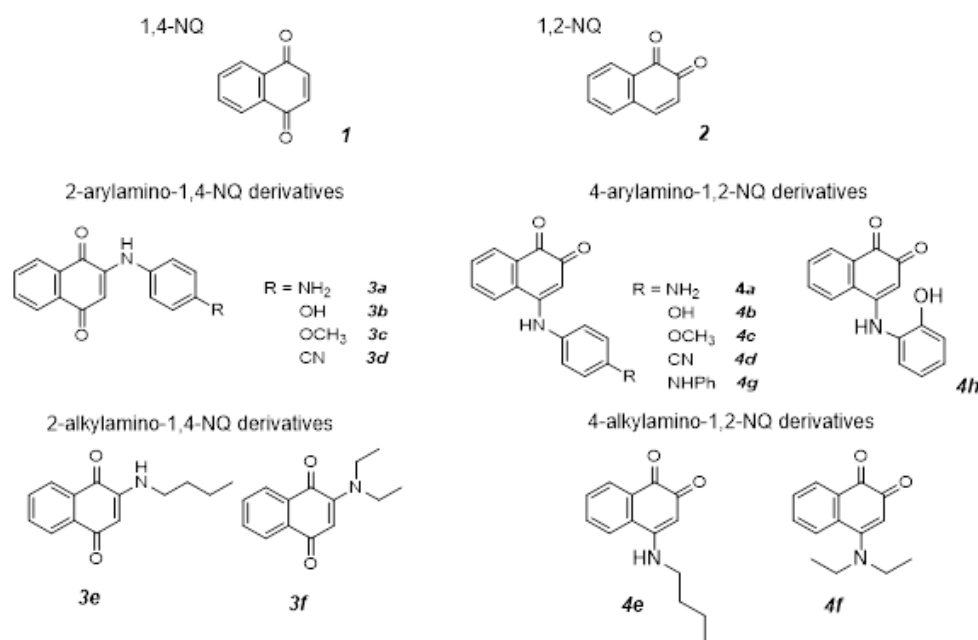


Figure 1. Structures of 1,4-NQ and 1,2-NQ and their derivatives.

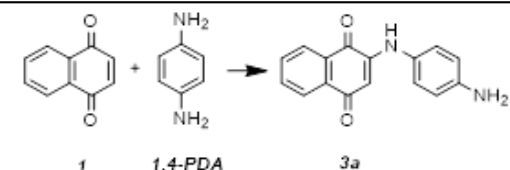
The synthesis of 2-substituted-1,4-naphthoquinone derivatives (**3a–f**) was performed by microwave-assisted reactions in the presence of a basic catalyst with moderate to excellent yields. The same approach was used for the 4-substituted-1,2-NQ derivatives (**4e,f** and **4h**) in the optimized experimental conditions. The 4-substituted-1,2-NQ derivatives (**4a–d** and **4g**) were obtained as previously reported by a biocatalytic strategy using CotA-laccase from *Bacillus subtilis* [32].

The experimental conditions for the MA reactions were optimized by an initial screening using equimolar quantities (50:50 mM) of 1,4-NQ (**1**) and 1,4-phenylenediamine (1,4-PDA) as a nucleophilic agent. A power of 200 W and a maximum temperature of 150 °C were set as microwave conditions, and experimental parameters such as different organic solvents, reaction times, and different catalysts were tested. The reactions were followed by HPLC (Figure S1, supplementary material), and the obtained conversion yields for **3a** are shown in Table 1.

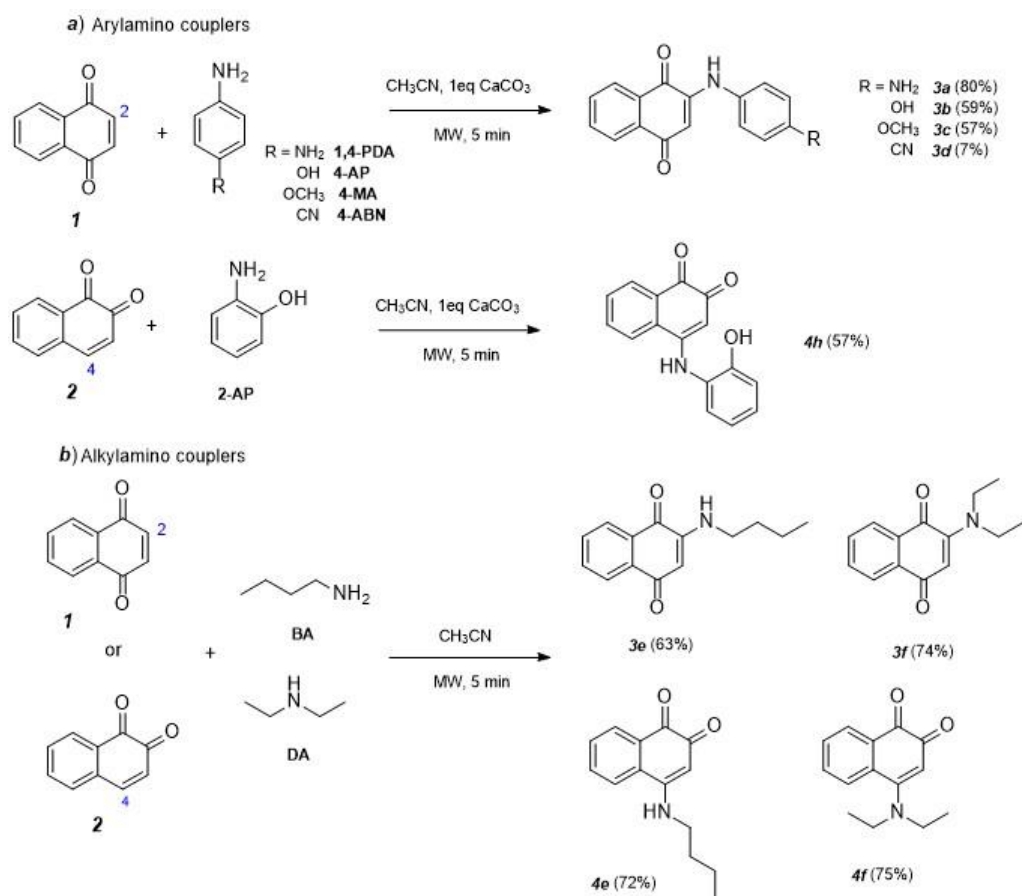
The reaction between 1,4-NQ (**1**) and 1,4-PDA yields **3a** (60%) after 10 min, in the absence of solvent (entry 2), and the introduction of different solvents (ethanol, acetonitrile, and acetone) did not improve the reaction yields (entries 4–8). Moreover, the use of a basic catalyst, CaCO₃, as a strategy to increase the nucleophilicity of the arylamine did not improve the yield (entry 3). However, the concomitant use of an organic solvent and a basic catalyst showed to be effective in the improvement of the reaction yield, particularly in the case of acetonitrile and CaCO₃ (entries 13–15). Other basic catalysts such as NaHCO₃ and K₂CO₃ were tested, in the presence and absence of solvent, without any product formation, as they cause degradation of 1,4-NQ starting material.

From these results, the following optimized experimental conditions were chosen: 5 min under 200 W microwave irradiation, at 150 °C, in 50:50 mM of 1,4-NQ:amine coupler with 1 eq. of CaCO₃, in acetonitrile:water (1:1), and different arylamines, namely, 4-aminophenol (4-AP), 4-methoxyaniline (4-MA) and 4-aminobenzonitrile (4-ABN) and the alkylamines, butylamine (BA) and diethylamine (DA) were selected, as nucleophiles, to prepare, by Michael 1,4-addition to position C-2, the analogues 2-arylamino-1,4-NQ (**3a–d**) and 2-alkylamino-1,4-NQ (**3e–f**), as shown in Scheme 1.

Table 1. Reactions yields for the synthesis of **3a** from 1,4-NQ and 1,4-PDA ¹.

Entry	Time (Min)			
		Solvent	Catalyst	Yield (%) ²
1	5	-	-	30
2	10	-	-	60
3	10	-	CaCO ₃	56
4	5	ethanol	-	26
5	10	ethanol	-	4
6	5	acetonitrile	-	14
7	10	acetonitrile	-	20
8	10	acetone	-	0
9	5	ethanol	CaCO ₃	68
10	10	ethanol	CaCO ₃	73
11	5	acetone	CaCO ₃	17
12	10	acetone	CaCO ₃	13
13	5	acetonitrile	CaCO ₃	76
14	10	acetonitrile	CaCO ₃	72
15	5	acetonitrile:water (1:1)	CaCO ₃	80

¹ Vt = 2 mL; p = 200 W, T = 150 °C. ² Determined by HPLC.

**Scheme 1.** MA synthesis of (a) 2-arylamines-1,4-NQ and 4-arylamines-1,2-NQ and (b) 2-alkylamines-1,4-NQ and 4-alkylamines-1,2-NQ.

The performance of the MA approach to the synthesis of derivatives **3a–f** was compared with conventional heating under similar experimental conditions (Table 2). Under MA conditions, good conversion yields (57–80%) were obtained for compounds **3a–c**, with the electron donor *p*-substituents enhancing the nucleophilicity of the aromatic amine. The yields are similar to or higher than the conventional reflux in comparatively shorter reaction times (Table 2), demonstrating that the effect of microwave irradiation is not purely thermal. As expected, due to the withdrawing nature of the CN group, compound **3d** was obtained in a low yield (7%). The same approach was used for the alkylamines (BA and DA), but the presence of CaCO₃ was revealed to have a negative effect, and compounds **3e–f** were synthesized in the absence of a catalyst (Table 2). Alkyl amines are more basic than aromatic amines, which justifies the good yields obtained for compounds **3e–f** in the absence of a catalyst (63 and 74%, respectively).

Table 2. Reaction yields of 2-*N*-arylamino-1,4-NQ derivatives (**3a–3f**) and *N*-alkylamino-1,4-NQ derivatives (**3e,f**) synthesized by conventional heating and MA protocols.

Compound	Coupler	Yield (%) ¹		
		MA ² + CaCO ₃ (1 Eq)	MA ²	Conventional Heating ³
3a	1,4-PDA	80	-	42 (2 h)
			-	61 (24 h)
			-	55 (2 h)
3b	4-AP	59	-	64 (4 h)
			-	67 (24 h)
			-	-
3c	4-MA	57	-	-
3d	4-ABN	7	-	0 (24 h)
3e	BA	54	63	62 (2 h)
				82 (4 h)
3f	DA	15	74	80 (24 h)
				-

¹ Determined by HPLC; ² V_t = 2 mL (1:1 CH₃CN:H₂O), P = 200 W, T = 150 °C; t = 5 min; ³ V_t = 50 mL (1:1 CH₃CN:H₂O), reflux.

The optimized MA conditions were used to prepare the 1,2-NQ derivatives (**4e**, **4f**, and **4h**) with the aliphatic amines and 2-aminophenol (2-AP), respectively (57–75%) (Scheme 1), showing that this approach can also be used to prepare this 4-substituted-1,2-NQ series. This last compound was prepared as a proof of concept to understand the influence of the position of the OH group in the aromatic amine.

The structures of synthesized compounds were assigned based on their ¹H and ¹³C NMR spectra and two-dimensional NMR (HSQC and HMBC) techniques. The ¹H NMR spectra of compounds **3a–f**, **4e–f**, and **4h** displayed comparable patterns whose signals multiplicity is in accordance with the proposed structures. Five characteristic signals described the naphthalene scaffold, two duplets (δ = 7.98–8.31 ppm), two triplets (δ = 7.59–7.82 ppm), and one singlet (δ = 5.68–6.22 ppm). The arylamine moieties on compounds **3a–d** are characterized by two duplets with resonances in the aromatic region (δ = 6.81–7.00 ppm) and for compound **4h** by two multiplets (δ = 6.90–7.40 ppm). For compounds **3e–f** and **4e–f**, with aliphatic amine substituents, the ¹H NMR spectra showed the characteristic signals in the aliphatic region (δ = 0.98–3.62 ppm). In the ¹³C NMR spectra, all carbon resonances were detected in the expected regions and assigned based on their chemical shifts and HSQC and HMBC cross signals. Furthermore, the structures were confirmed by ESI-MS spectrometry in accordance with their molecular formula. The mass spectra of all products exhibit the correspondent signals to the protonated molecules [M + H]⁺ at *m/z* 265, 266, 280, 275, 266 for **3a–d** and **4h** and *m/z* 230 for **3e,f** and **4e,f**, respectively. Generally, for all ions, the first fragmentation pattern [ESI(+)-MS²] is consistent with the correspondent typical loss of CO leading to signals [M+1–CO]⁺.

2.2. Electrochemistry Studies

Electron transfers play important roles in the bioactivation of redox-active drugs, in their metabolism/catabolism, and in their targeted release at precise destinations and frequently promoted their ligand-target interactions. Redox potentials provide information on the feasibility of electron transfer *in vivo* and established relationships between the ease of reduction (represented by E_{pc} or $E_{1/2}$) and biological activities, demonstrating the relevance of electrochemical studies as tools for the comprehension of drug mechanism of action against various diseases, for the prediction of biological activities and for the design of potentially active compounds [6,33–35].

To obtain an insight into the electronic character of the studied naphthoquinone derivatives and to find out possible relationships with their potential biological activities, the electrochemical behavior of 1,4-NQ (1) and 1,2-NQ (2) and their 2-substituted-1,4-NQ (3a–f) and 4-substituted-1,2-NQ derivatives (4a–h), respectively, were studied by cyclic voltammetry (CV) in aprotic medium ($\text{CH}_3\text{CN} + \text{TBAP}$, 0.1 mol.L^{-1}) and the electrochemical selected data are listed in Table 3 (for complete electrochemical data, see Tables S1 and S2, supplementary material).

Table 3. Selected electrochemical data in acetonitrile (scan rate: $0.100 \text{ V}\cdot\text{s}^{-1}$).

Compound	E_{pc} (I) (V) ($E_{1/2}$; ΔE (mV))	E_{pc} (II) (V) ($E_{1/2}$; ΔE (mV))
1,4-NQ (1)	−0.70 (−0.66; 80)	−1.36
3a	−0.86 (−0.82; 80)	−1.42
3b	−0.84 (−0.81; 70)	−
3c	−0.86 (−0.82; 70)	−1.34
3d	−0.74 (−0.70; 80)	−
3e	−0.98 (−0.95; 70)	−1.47 (−1.42; 100)
3f	−0.97 (−0.94; 70)	−
1,2-NQ (2)	−0.55 (−0.50; 110)	−0.98 (−0.91; 140)
4a	−0.67	−
4b	−0.61	−
4c	−0.67	−
4d	−0.47	−0.84
4g	−0.63	−1.43
4h	−0.57	−0.98
4e	−0.78	−
4f	−0.52	−0.69 (−0.63, 120)

The cyclic voltammogram of the precursor, 1,4-NQ (1) (Figure 2a), shows the presence of two sequential mono-electronic reductive waves, being the first one quasi-reversible ($E_{pc}(I) = -0.70 \text{ V vs. SCE}$, $E_{1/2} = -0.66 \text{ V}$) and the second, broader and less-defined, irreversible ($E_{pc}(II) = -1.36 \text{ V}$). In order to estimate the contribution of the relative position of the quinonoid groups to the electrochemical response, the 1,2-NQ (2) was also studied in the same conditions (Figure 2b). Similarly, the 1,2-NQ (2) shows two sequential mono-electronic quasi-reversible waves ($E_{pc}(I) = -0.55 \text{ V}$, $E_{1/2} = -0.50 \text{ V}$; $E_{pc}(II) = -0.98 \text{ V}$). They correspond, as already known, the first pair to the generation of the semiquinone ($\text{SNQ}^{\bullet-}$), followed, in the second step, by the dianion (NQ^{2-}) formation [6–8]. Thus, 1,2-NQ is easier to be reduced than 1,4-NQ being this behavior is observed in both reductive steps.

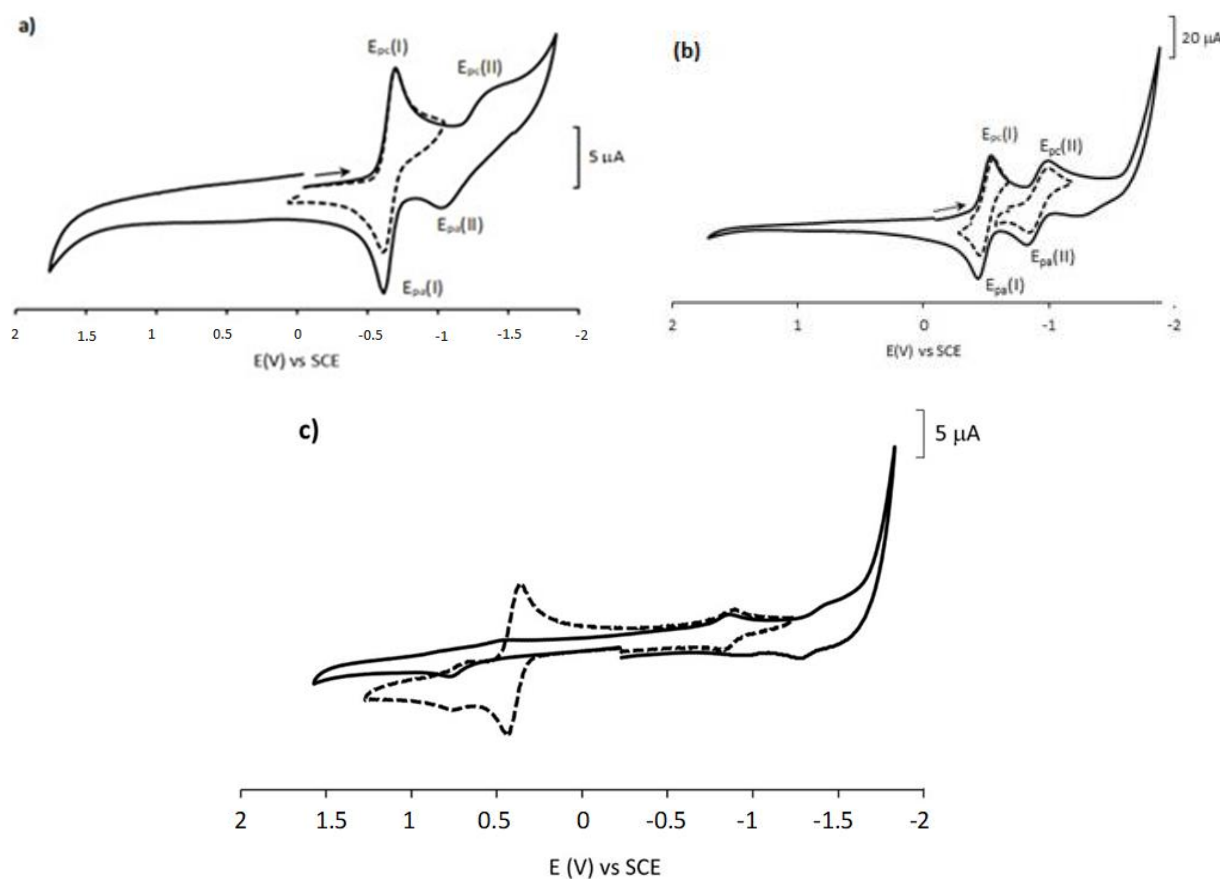


Figure 2. Cyclic voltammograms of (a) 1,4-NQ, showing the isolated redox process (dashed line); (b) 1,2-NQ showing the isolated redox process (dashed line) and (c) **3a** in ACN + TBAPF₆ (black line), showing the isolated redox processes and ferrocene redox pair (dashed line), at the scan rate of 0.1 V·s⁻¹.

The influence of substituents on the electrochemical properties of 1,4-NQ and 1,2-NQ was also studied for both series and the CV of **3a**, the most cytotoxic 1,4-NQ derivative is shown, as an example, in Figure 2c. The electrochemical data of the other 2-substituted-1,4-NQ derivatives are similar (data in Table 3). The redox profile showed the following two independent systems: the reduction of the naphthoquinone moiety and the oxidation of the amine substituent moiety in the anodic part (Figure 2c). The redox processes displayed in the range +0.72 to +1.55 V were related to oxidations within the substituted anilines or aliphatic amines. The substitution at the 1,4-NQ moiety generally leads to easier oxidations when compared with the correspondent 1,2-NQ. Analysis of the cathodic region showed one or two reductive processes for the 1,4-NQ and 1,2-NQ nucleus, shifted to lower potential values and less reversible upon substitution with the aromatic or aliphatic amines. The ease of reduction, represented by the potential of the first well-defined wave ($E_{pc}(I)$), for both NQ series follows the following order: CN > OH ~ NHPH > OCH₃ ~ NH₂ > Diethylamine ~ Butylamine. In the 1,4-NQ series, a difference of 240 mV was observed between compound **3d**, the most easily reduced, and the butylamine derivative (**3e**), reduced at more negative potentials. For the 1,2-NQ series, the difference is even higher (310 mV) between **4d** and **4e**. Generally, the trend observed on the redox potentials is clearly related to the electronic effects of the substituents. Aliphatic amine substituents **3e**, **3f**, **4e**, and **4f** exhibit the lowest redox potentials indicating that the aliphatic amino groups decreased the electron affinity of the naphthoquinone scaffolds. Electron donors or withdrawing substituents within the amine aromatic ring directly influence the electron density of the 1,2- and 1,4-NQs moieties. While 1,4-NQ or 1,2-NQ with electron-donating substituents such as NH₂, OH, and OCH₃ have comparatively low values, the electron-withdrawing CN shows no appreciable change, being, therefore, easier to reduce.

2.3. In Silico Studies

As a first approach, the Molinspiration cheminformatics program [36] was used to predict the in silico molecular properties of the 2-substituted-1,4-NQ and 4-substituted-1,2-NQ derivatives. The theoretical oral bioavailability was predicted using the “Rule of five” proposed by Lipinski and Lombardo [37] and the percentage of oral absorption (ABS%) [38] (see Tables S3 and S4). The bioactivity scores were estimated for drug targets, such as G-protein coupled receptor ligands, ion channel modulators, kinase inhibitors, nuclear receptor ligands, protease inhibitors, and enzyme inhibitors, and results were summarized in Table S5 (see supplementary material).

Based on the results, all compounds showed adequate molecular properties and met the criteria established by Lipinski’s “rule of five”, presenting adequate hydrophobic properties ($\log P \leq 5$, exception for compound **4g**), size properties ($M \leq 500$ g/mol and $TPSA \leq 140$ Å) and bond restrictions ($n_{OH} \leq 10$ and $n_{OHNH} \leq 5$). Furthermore, the calculated ABS% (from 84.6 to 99.4% range) suggests good membrane permeability for the compounds. Regarding the predicted bioactivity scores against common molecular targets, the results clearly indicate an improvement in the bioactivity scores upon the substitution of 1,2-NQ and 1,4-NQ scaffolds. In particular, the results showed that both 2-aryl-1,4-NQs and 4-aryl-1,2-NQs are expected to be biologically active as kinase inhibitors (see Table S5). In fact, the 1,4-NQ skeleton and other quinone-derived compounds had already been reported as active against kinases, by biochemical binding and molecular interaction with the kinases catalytic sites [39]. Kinase inhibitors are a large group of antineoplastic agents targeting protein kinases, which are altered in cancer cells leading to abnormal growth; hence, kinase inhibitors are considered a promising approach for anticancer drug development [40].

2.4. Biological Assays

2.4.1. In Vitro Cytotoxicity against Human Hepatocarcinoma Cell Line HepG2

The potential in cancer therapy showed by natural and synthetic naphthoquinones derivatives [9–11] and the predicted biological activity as kinase inhibitors provided by in silico studies prompted us to determine the cytotoxicity profile of substituted 1,4-NQ and 1,2-NQ derivatives (**3a–f** and **4a–h**) together with 1,4-NQ and 1,2-NQ.

A hepatocellular carcinoma cell line HepG2, recognized for studying the metabolism of anticancer drugs, was used [41]. The viability of HepG2 cell line culture after 24 h incubation with the compounds using the MTT (3-[4,5-dimethylthiazol-2-yl]-2,5-diphenyl tetrazolium bromide) assay [42,43] was evaluated, and doxorubicin (**Doxo**) was used as a positive control. A dose-dependent cytotoxic effect was observed for all compounds (see supplementary material, Figures S15 and S16), the effective concentration of each compound (μM) leading to the death of 50% of the cells (EC_{50}) was calculated, and the results are presented in Figure 3 (see also Table S6).

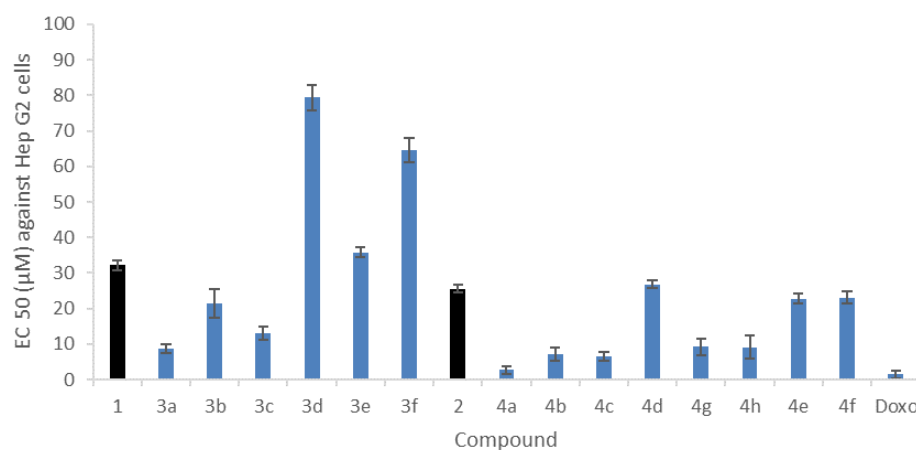


Figure 3. EC_{50} values for the cytotoxicity of compounds **1**, **2**, **3a–f**, **4a–f**, and **Doxo**. EC_{50} values were calculated using Graph Pad Prism and expressed as the mean \pm SD.

All compounds showed cytotoxic activity in the μM range and inhibited cell proliferation of the HepG2 cell line. These results additionally showed that 1,2-NQ derivatives (**4a–f**) exhibit a stronger effect than their 1,4-NQ homologues (**3a–f**). Derivatization with 4-substituted aromatic amines with donor groups leads to an improvement in the cytotoxic potential, with EC_{50} values ranging from 9 to 21 μM for **3a–c** and from 3 to 7 μM for **4a–c** when compared to their respective precursors 1,4-NQ ($\text{EC}_{50} = 32 \mu\text{M}$) and 1,2-NQ ($\text{EC}_{50} = 26 \mu\text{M}$), respectively. Derivatization with 4-substituted aromatic amine with a cyano group (**3d** and **4d**) and with N-alkyl amines (**3e–f** and **4e–f**) decreases the cytotoxicity for both precursors. The highest cytotoxic activity was found for compound **4a** ($\text{EC}_{50} = 3 \mu\text{M}$), which is a promising result when compared to doxorubicin ($\text{EC}_{50} = 1.4 \mu\text{M}$) used as a positive control.

The cytotoxic activity of these compounds can be related to their electrochemical properties, for which the experimental data showed that overall, the 1,2-NQ derivatives present higher reductive potentials (E_{pc}) than their 1,4-NQ homologues and consequently a stronger oxidizing power, which may justify its cytotoxic effect. It has been postulated that the cytotoxicity is mediated through semiquinone radical species, which are formed during the quinone conversion and vice-versa and thus is highly dependent on the electrochemical potential of the initially formed radical species [34,44]. The anticancer agent doxorubicin and other quinones are also known to cause chemical and oxidative damage to cells [45].

2.4.2. Inhibition of Acetylcholinesterase Activity

The acetylcholinesterase enzyme (AChE, EC 3.1.1.7) plays a major role in the activity of the central and peripheral nervous systems, and its inhibition represents an important therapeutic target for AD [23]. The adverse effects shown by AChEIs in use in the treatment of Alzheimer's and dementia symptoms [24], the growing importance of neurodegenerative diseases, and previous studies on naphthoquinones as AchEIs [21] led us to extend our studies to the potential for inhibition of AchE activity.

The inhibitory activities against AchE were evaluated for all compounds at a concentration of 50 μM , and the $\text{Inhibition}_{50\mu\text{M}}$ values are given in Figure 4 (see also Table S7).

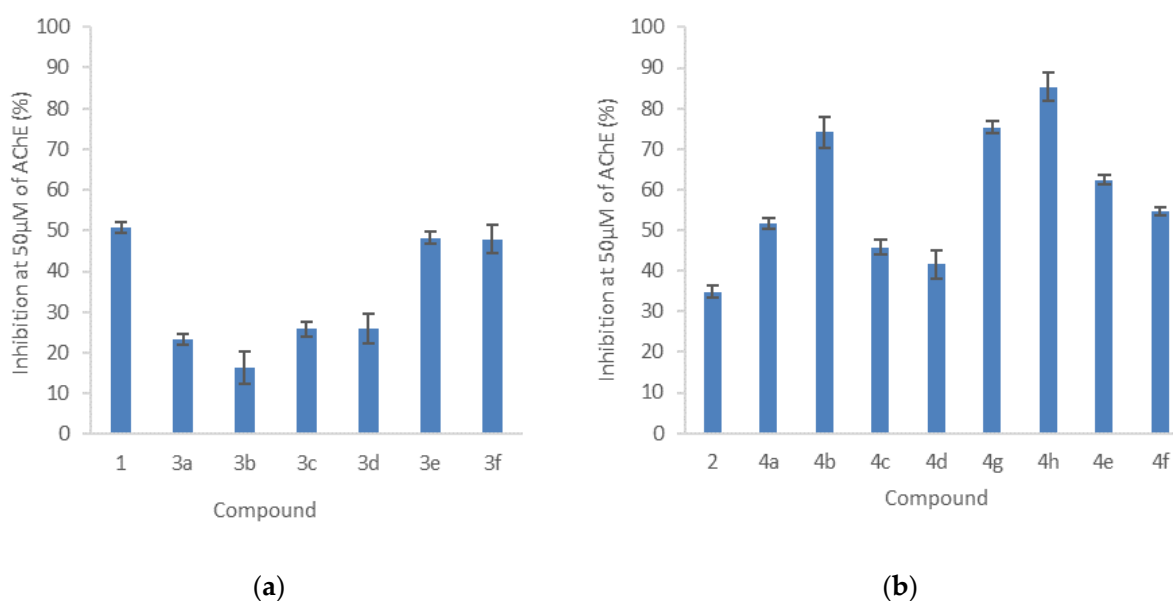


Figure 4. Inhibitory activities against AChE at a concentration of 50 μM — $\text{Inhibition}_{50\mu\text{M}}$ values for (a) 1,4-NQ and their derivatives **3a–f**; (b) 1,2-NQ and their derivatives **4a–h**. Values were calculated using Graph Pad Prism and expressed as the mean \pm SD.

Results show that 1,4-NQ (**1**) and 1,2-NQ (**2**) exhibit AChE inhibitory values for a concentration of 50 μM of 51% and 35%, respectively. As shown in Figure 4, different trends

are observed after substitution with aryl- or alkylamines. The 2-substituted-1,4-NQ derivatives (**3a–f**) decrease the 1,4-NQ inhibitory activity against AChE (Figure 4a), whereas 4-substituted-1,2-NQ derivatives (**4a–f**) showed an increase in the potential shown by 1,2-NQ (Figure 4b). Thus, the 1,2-NQ derivatives (**4a–f**) showed moderate inhibition to AChE, with compound **4h** presenting the highest AChE inhibitory activity (Inhibition_{50 μ M} = 85%). In fact, when the position of the hydroxyl group changes from para (**4b**) to ortho (**4h**) position, a slight increase in the inhibitory activity against AChE was observed.

Additionally, a dose-dependent AChE inhibition effect was determined for all, and the effective concentration of each compound (μ M) that leads to the 50% of enzyme inhibition (AChEIC₅₀) was calculated for compounds **4b** (30 μ M) and **4h** (16 μ M). These values, higher than the AChEIC₅₀ values of the reference AChE inhibitors rivastigmine (1.03 μ M) or galantamine (1.99 μ M) [46], show that these compounds are only moderate AChE inhibitors and further structural changes must be considered for these 1,2-NQ and 1,4-NQ families can be foreseen as alternative drug scaffolds.

2.5. Molecular Docking Studies

Molecular docking studies were performed to further elucidate the binding interactions between the 1,2-NQ derivative **4b**, the most potent AChE inhibitor, and the corresponding 1,4-NQ derivative **3b**, with poorer performance, and AChE enzyme active site gorge. The molecular docking studies were performed with AutoDock Vina v.1.2.0 software. Based on the docking score, the best conformation of the compounds binding at the AChE active site gorge was chosen, and the interactions of 1,4-NQ derivative **3b** and 1,2-NQ derivative **4b** with AChE are shown in Figure 5. Bond types and distances are summarized in Tables S8 and S9 (see supplementary materials).

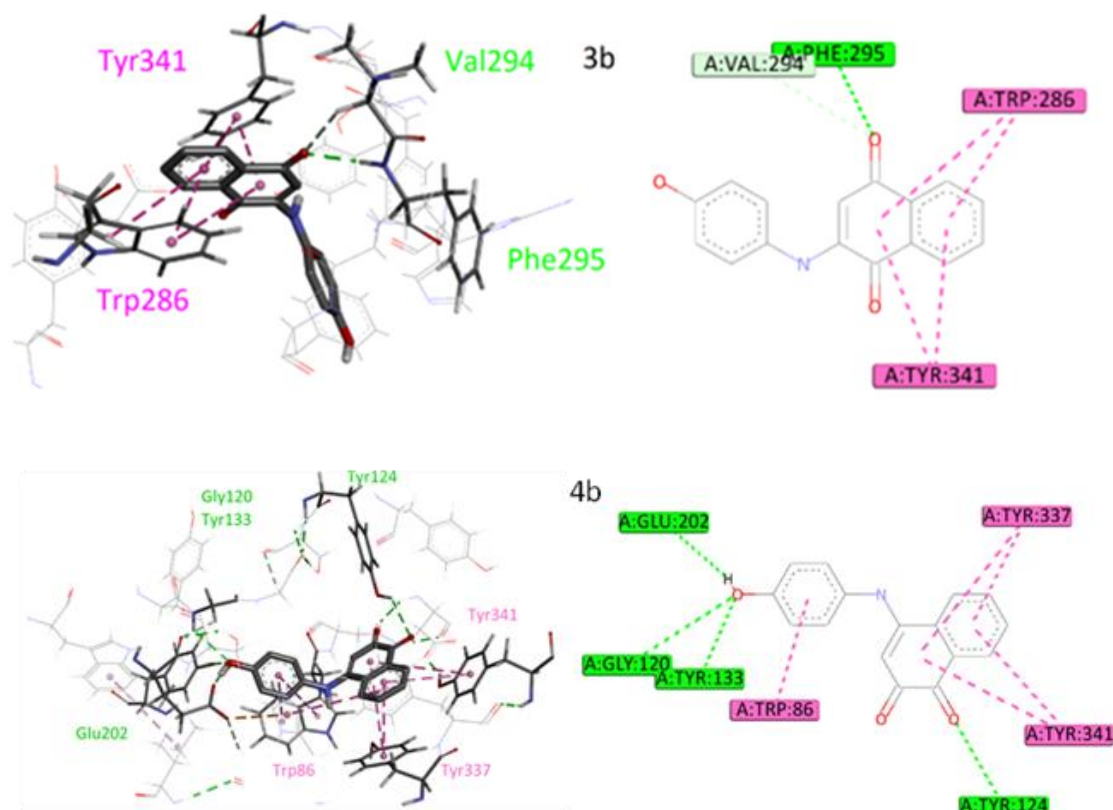


Figure 5. Binding mode prediction for compounds **3b** and **4b** with AChE (PDB id:4EY7) visualized in Discovery Studio, BIOVIA. Color coding: pink, π - π aromatic interaction; green, conventional hydrogen bond.

The docking results showed that both compounds fit well in the binding pocket of AChE, and hydrogen bond and π - π stacking interactions were found between both compounds and the amino acid residues at the AChE gorge. As depicted in Figure 5, the 1,4-NQ derivative **3b** shows one hydrogen bond between one quinonoid carbonyl group and the Phe295 residue located at the mid-gorge. Both aromatic rings of the 1,4-NQ scaffold stack with the aromatic residues, Trp286 and Tyr341, belong to the peripheral anionic site (PAS), which is situated near the entrance of the gorge. Moreover, the NQ ring of **3b** also showed an additional hydrogen bond with Val294 located at the entrance of the AChE active site. Both the hydroxyl group and the peripheric aromatic ring of **3b** were not involved in any interactions. A molecular docking study of the 1,2-NQ derivative **4b** (Figure 5) showed a hydrogen bond involving the quinonoid carbonyl group and Tyr124 residue located at the PAS region. In addition, the Tyr341 residue at PAS region interacts via arene-arene stacking with **4b**. Other strong hydrogen bonds were observed between the hydroxyl group of the peripheric aromatic ring and Tyr133 residue on the catalytic anionic site (CAS) and Glu202, one of the acidic amino acids surrounding the CAS region, located at the bottom of the gorge and near the AChE catalytic triad. Other crucial amino acids at the CAS region, Trp86, and Tyr337 residues, interact via important π - π stacking interactions with all the aromatic rings present on **4b**. The CAS site is involved in the binding of the choline moiety of ACh and the residues Trp86 and Tyr337 were seen to be critical for the inhibition of AChE [47].

In general, the major difference between the two compounds, **3b** and **4b**, is related to the fact that the 1,4-NQ derivative (**3b**) showed interactions between the NQ ring, the PAS, and mid-gorge regions, whereas the 1,2-NQ derivative (**4b**) interacts with the PAS region and additionally, by the NQ ring and the peripheric aromatic substituent, with several amino acid residues nearby the CAS region. The importance of these interactions with CAS residues was reinforced by the docking results obtained for derivative **4h**. This 1,2-NQ derivative showed several interactions within the CAS region surrounding residues (Trp86, Tyr133 and Tyr337) both by hydrogen bond and π - π stacking interactions (Table S10, supplementary material).

Comparison of the docking results from compounds **4b** and **4h** (Figure 6) evidence that both compounds at the AChE active site interact with residues at PAS and CAS.

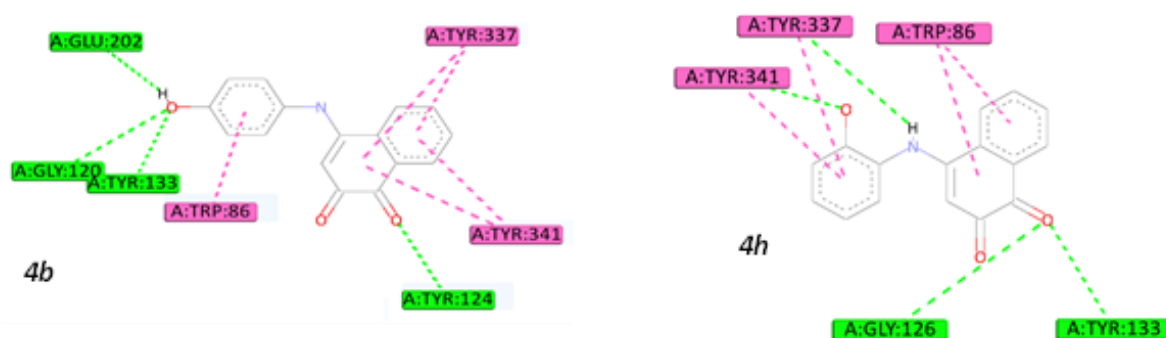


Figure 6. Binding mode prediction for compounds **4b** and **4h** with AChE (PDB id:4EY7) visualized in Discovery Studio, BIOVIA. Color coding: pink, π - π aromatic interaction; green, conventional hydrogen bond.

This strong hydrogen binding and hydrophobic interaction with the active site residues of AChE may be one of the reasons for the good inhibitory activity shown by the 1,2-NQ derivative compounds in the series. Dual-binding cholinesterase inhibitors, such as donepezil, have been reported to interact with both CAS and PAS regions, and these interactions were reported to be related to their potent AChE inhibition profiles [47–49].

3. Materials and Methods

Microwave-assisted syntheses were performed with a CEM Discover SP microwave synthesizer system (2.45 GHz, 300 W, CEM Microwave Technology Ltd., Buckingham, UK) equipped with a non-contact infrared temperature sensor. Experiments were performed in sealed Pyrex microwave vials using dynamic mode and the reaction temperature was controlled by variable microwave irradiation (0–200 W) and cooling by nitrogen current.

Reagents and solvents were purchased from Merck (Darmstadt, Germany) or Alfa Aesar (Kandel, Germany) with high purity and used without further purification. Analytical thin-layer chromatography (TLC) was performed using silica gel 60 F254 precoated plates (0.25 mm thickness) with a fluorescent indicator. Column chromatography was carried out using silica gel 60 (EM Separations Technology) as the stationary phase. ^1H and ^{13}C NMR spectra were obtained in $\text{CD}_3\text{OD}-d_4$ as solvent using a Bruker Avance 400 MHz spectrometer (Bruker, Billerica, MA, USA) with a 5 mm probe. Chemical shifts (δ) are given in ppm and reported based on TMS as standard. Spin multiplicities are given as s (singlet), d (doublet), t (triplet), and m (multiplet). Coupling constants (J) are in Hz. Spectra are reported as follows: chemical shift (δ , ppm), multiplicity, integration, and coupling constants (Hz).

HPLC was conducted on a Waters Alliance e2695 Separations Module (Massachusetts, EUA) with 2489 UV/Vis Detector, also from Waters. The chromatographic separation was conducted with a Symmetry C18 column (250 \times 4.6 mm, 5 μm ; Waters), with formic acid 0.1% (*v/v*) and acetonitrile as mobile phases A and B, respectively. A 32-min linear gradient from 5 to 70% of acetonitrile mobile phase B, followed by an 8-min linear gradient to 100% of mobile phase B, was used in all instances. The injection volume was 10 μL , and the detection was performed at 270 nm.

Low-resolution mass spectra were recorded on an LCQ Fleet, Thermo Scientific Ion Trap mass spectrometer, operated in the electrospray ionization (ESI) positive/negative ion modes. The optimized parameters were as follows: ion spray voltage, ± 4.5 kV; capillary voltage, +16 and -20 V; tube lens offset, -63 and $+82$ V; sheath gas (N_2), 80 arbitrary units; auxiliary gas, 5 arbitrary units; capillary temperature, 250°C . The spectra were recorded in the range of 50–1000 Da. Spectrum typically corresponds to the average of 20–35 scans. Sequential mass spectra were obtained with an isolation window of 2 Da, a 25–30% relative collision energy and with an activation energy of 30 msec. High-resolution ESI (+/–) mass spectra were obtained on a QTOF Impact IITM mass spectrometer (Bruker Daltonics, GMBH; Germany), operating in the high-resolution ion mode. Calibration of the TOF analyzer was performed with a 10 mM sodium formate calibrant solution. Data were processed using Data Analysis 4.2 software.

The redox potentials were measured by cyclic voltammetry using an EG&G Princeton Applied Research (PAR) Model 273A potentiostat/galvanostat monitored by a personal computer with the Electrochemistry PowerSuite v2.51 software from PAR. Cyclic voltammograms were obtained in 1 mM of compounds in anhydrous acetonitrile solutions containing tetrabutylammonium hexafluorophosphate (TBAPF_6) 0.1 M as supporting electrolyte. A three-electrode configuration cell was used with a homemade platinum disk working electrode (1.0 mm diameter) probed by a Luggin capillary connected to a silver-wire pseudo-reference electrode and a platinum wire auxiliary electrode. The potentials were scanned from -1.8 to 1.8 V at a scan rate of $100\text{ mV}\cdot\text{s}^{-1}$. All measurements were done at room temperature and the solutions were deaerated with nitrogen atmosphere before use. All the potentials reported were measured against the ferrocene/ferrocenium redox couple as internal standard and corrected to SCE (using the ferrocenium/ferrocene redox couple $E_{1/2} = 0.40$ V vs. SCE).

3.1. Optimized Conditions for Microwave-Assisted Synthesis of 1,4-NQ Derivatives (3a–d)

The 1,4-naphthoquinone (**1**) (15.8 mg, 50 μmol) and aryl amines (1,4-PDA, 4-AP, 4-MA, and 4-ABN) (50 μmol) were dissolved in acetonitrile (1 mL) in a microwave vial. In total, 1 mL of CaCO_3 aqueous solution (50 μmol) was added and the vial sealed. The

resulting solution was stirred under microwave irradiation (200 W) at 150 °C for 5 min. After cooling, products (**3a–d**) were extracted with ethyl acetate. Solvent was evaporated under reduced pressure and residues purified by column chromatography (silica gel, ethyl acetate:chloroform 1:3).

2-(1,4-Phenylenediamine)-1,4-naphthoquinone (3a): Purple solid (80%): ^1H NMR (400 MHz, MeOD- d_4): δ (ppm) = 8.11 (d, 1H, J = 7.2 Hz, H5), 8.02 (d, 1H, J = 7.5 Hz, H8), 7.80 (t, 1H, J = 7.8 Hz, H7), 7.72 (t, 1H, J = 7.4 Hz, H6), 7.09 (d, 2H, J = 8.6 Hz, H12, H16), 6.81 (d, 2H, J = 8.6 Hz, H13, H15) and 6.01 (s, 1H, H3). ^{13}C NMR (100 MHz, MeOD- d_4): δ (ppm) = 185.5 (C4), 183.0 (C1), 147.8 (C2), 135.9 (C7), 134.8 (C10), 133.5 (C6), 132.1 (C9), 127.5 (C5), 126.8 (C8), 126.5 (C12, C16), 116.9 (C13, C15) and 101.4 (C3). ESI-MS positive mode: 287 [M+Na] $^+$; 265 [M+H] $^+$, MS 2 (m/z): 237 [M+H-CO] $^+$, MS 3 (m/z): 209 [M+H-CO-CO] $^+$; ESI-MS negative mode: 263 [M-H] $^-$. ESI-HRMS: m/z calcd. for [C $_{16}$ H $_{13}$ N $_2$ O $_2$ +H] $^+$: 265.0972; found 265.0980.

2-(4-aminophenol)-1,4-naphthoquinone (3b): orange solid (59%): ^1H NMR (400 MHz, MeOD- d_4): δ (ppm) = 8.11 (d, 1H, J = 7.7 Hz, H5), 8.02 (d, 1H, J = 7.6 Hz, H8), 7.80 (t, 1H, J = 7.5 Hz, H7), 7.70 (t, 1H, J = 7.5 Hz, H6), 7.17 (d, 2H, J = 8.8 Hz, H12, H16), 6.87 (d, 2H, J = 8.8 Hz, H13, H15) and 6.0 (s, 1H, H3). ^{13}C NMR (100 MHz, MeOD- d_4): δ (ppm) = 185.6 (C4), 182.9 (C1), 157.2 (C14), 135.9 (C7), 133.6 (C6), 132.1 (C10), 130.4 (C9), 127.4 (C5), 126.9 (C12, C16), 126.8 (C8), 117.1 (C13, C15) and 101.7 (C3). ESI-MS positive mode: 266 [M+H] $^+$, MS 2 (m/z): 238 [M+H-CO] $^+$. ESI-HRMS: m/z calcd. for [C $_{16}$ H $_{11}$ NO $_3$ +H] $^+$: 266.0812; found 266.0810.

2-(4-methoxyaniline)-1,4-naphthoquinone (3c): brown solid (57%): ^1H NMR (400 MHz, MeOD- d_4): δ (ppm) = 8.09 (d, 1H, J = 7.6 Hz, H5), 8.00 (d, 1H, J = 7.7 Hz, H8), 7.78 (t, 1H, J = 7.5 Hz, H7), 7.70 (t, 1H, J = 7.5 Hz, H6), 7.25 (d, 2H, J = 8.8 Hz, H12, H16), 7.00 (d, 2H, J = 8.8 Hz, H13, H15), 6.02 (s, 1H, H3) and 3.82 (s, 3H, CH $_3$). ^{13}C NMR (100 MHz, MeOD- d_4): δ (ppm) = 185.6 (C4), 182.8 (C1), 159.4 (C14), 135.8 (C7), 133.6 (C6), 133.2 (C10), 132.1 (C9), 129.4 (C11), 127.4 (C5), 126.8 (C8), 126.7 (C12, C16), 115.8 (C13, C15), 101.9 (C3) and 56.0 (CH $_3$). ESI-MS positive mode: 280 [M+H] $^+$, MS 2 (m/z): 252 [M+H-CO] $^+$. ESI-HRMS: m/z calcd. for [C $_{17}$ H $_{13}$ NO $_3$ +H] $^+$: 280.0968; found 280.0976.

2-(4-aminobenzonitrile)-1,4-naphthoquinone (3d): orange solid (7%): ^1H NMR (400 MHz, MeOD- d_4): δ (ppm) = 8.31 (d, 1H, J = 7.8 Hz, H5), 8.05 (d, 1H, J = 7.8 Hz, H8), 7.82 (t, 1H, J = 7.2 Hz, H7), 7.65 (t, 1H, J = 7.2 Hz, H6), 7.48 (d, 2H, J = 9.0 Hz, H12, H16), 7.35 (d, 2H, J = 9.0 Hz, H13, H15), 6.22 (s, 1H, H3). ESI-MS positive mode: 275 [M+H] $^+$, MS 2 (m/z): 247 [M+H-CO] $^+$. ESI-HRMS: m/z calcd. for [C $_{17}$ H $_{10}$ N $_2$ O $_2$ +H] $^+$: 275.0815; found 275.0819.

3.2. Optimized Conditions for Microwave Synthesis of 1,4-NQ Derivatives (**3e,f**) and 1,2-NQ Derivatives (**4e,f**)

The 1,4-naphthoquinone (**1**) or 1,2-naphthoquinone (**2**) (15.8 mg, 50 μmol) and alkyl amines (BA and DA) (50 μmol) were dissolved in acetonitrile (2 mL) and the microwave vial was sealed. Solution was stirred under microwave irradiation (200 W) at 150 °C for 5 min. After cooling, products were extracted with ethyl acetate. Solvent was evaporated under reduced pressure and residues purified by column chromatography (silica gel, ethyl acetate:chloroform 1:3).

2-(butan-1-amine)-1,4-naphthoquinone (3e): orange solid (63%): ^1H NMR (400 MHz, MeOD- d_4): δ (ppm) = 8.01 (dd, 2H, J = 6.9 Hz, H5, H8), 7.75 (t, 1H, J = 7.5 Hz, H7), 7.66 (t, 1H, J = 7.5 Hz, H6), 5.68 (s, 1H, H3), 3.23 (t, 2H, J = 7.2 Hz, H11), 1.66 (d, 2H, J = 7.4 Hz, H12), 1.44 (d, 2H, J = 7.4 Hz, H13) and 0.98 (t, 3H, J = 7.3 Hz, H14). ^{13}C NMR (100 MHz, MeOD- d_4): δ (ppm) = 184.7 (C4), 182.6 (C1), 150.8 (C2), 135.8 (C7), 135.0 (C9), 133.3 (C6), 132.1 (C10), 127.3 (C8), 126.8 (C5), 99.9 (C3), 43.2 (C11), 31.1 (C12), 21.3 (C13) 14.1 (C14). ESI-MS positive mode: 230 [M+H] $^+$. ESI-HRMS: m/z calcd. for [C $_{14}$ H $_{15}$ NO $_2$ +H] $^+$: 230.1176; found 230.1180.

2-(diethylamine)-1,4-naphthoquinone (3f): red solid (74%): ^1H NMR (400 MHz, MeOD- d_4): δ (ppm) = 7.98 (dd, 2H, J = 7.9 Hz, H5, H8), 7.76 (t, 1H, J = 7.4 Hz, H7), 7.68 (t, 1H, J = 7.4 Hz, H6), 5.86 (s, 1H, H3), 3.62 (m, 2H, H11) and 1.32 (t, 2H, J = 7.0 Hz, H12). ^{13}C NMR (100 MHz, MeOD- d_4): δ (ppm) = 184.7 (C4), 184.4 (C1), 153.3 (C2), 135.0 (C7), 134.3 (C9), 134.1 (C10),

133.3 (C6), 125.9 (C5, C8), 105.0 (C3), 48.0 (C11, C11') and 12.9 (C12, C12'). ESI-MS positive mode: 230 [M+H]⁺. ESI-HRMS: *m/z* calcd. for [C₁₄H₁₅NO₂+H]⁺: 230.1176; found 230.1177. 4-(butan-1-amine)-1,2-naphthoquinone (**4e**): red solid (72%): ¹H NMR (400 MHz, MeOD-d₄): δ(ppm) = 8.12 (d, 1H, *J* = 8.0 Hz, H8), 8.05 (d, 1H, *J* = 8.0 Hz, H5), 7.80 (t, 1H, *J* = 8.0 Hz, H6), 7.70 (t, 1H, *J* = 8.0 Hz, H7), 5.90 (s, 1H, H3), 3.52 (t, 2H, *J* = 8.0 Hz, H11), 1.76 (d, 2H, *J* = 7.4 Hz, H12), 1.48 (d, 2H, *J* = 8.0 Hz, H13) and 1.00 (t, 3H, *J* = 8.0 Hz, H14). ¹³C NMR (100 MHz, MeOD-d₄): δ(ppm) = 180.9 (C1), 175.3 (C2), 159.4 (C4), 135.8 (C7), 135.6 (C6), 132.9 (C7), 132.6 (C10), 131.9 (C9), 129.3 (C8), 124.6 (C5), 98.9 (C3), 44.9 (C11), 31.5 (C12), 21.3 (C13) 14.1 (C14). ESI-MS positive mode: 256 [M+Na]⁺ and 230 [M+H]⁺. ESI-HRMS: *m/z* calcd. for [C₁₄H₁₅NO₂+H]⁺: 230.1176; found 230.1183.

4-(diethylamine)-1,2-naphthoquinone (**4f**): red solid (75%): ¹H NMR (400 MHz, MeOD-d₄): δ(ppm) = 8.05 (dd, 2H, *J* = 7.9 Hz, H5, H8), 7.75 (t, 2H, *J* = 7.4 Hz, H6, H7), 6.02 (s, 1H, H3), 3.68 (q, 4H, H11, H11') and 1.41 (t, 6H, *J* = 8.0 Hz, H12, H12'). ¹³C NMR (400 MHz, MeOD-d₄): δ(ppm) = 183.7 (C1), 177.6 (C2), 165.6 (C4), 135.0 (C6), 133.3 (C9), 132.4 (C5), 130.2 (C10), 129.9 (C9), 129.9 (C8), 128.7 (C7), 105.4 (C3), 47.9 (C11, C11') and 13.0 (C12, C12'). ESI-MS positive mode: ESI-MS positive mode: 256 [M+Na]⁺ and 230 [M+H]⁺. ESI-HRMS: *m/z* calcd. for [C₁₄H₁₅NO₂+H]⁺: 230.1176; found 230.1176.

3.3. Bioactivity Score Prediction

Drug score values indicate the overall potential of a compound to be a drug candidate. Mol inspiration is a web-based tool used to predict the bioactivity score of synthesized compounds against regular human receptors such as GPCRs, ion channels, kinases, nuclear receptors, proteases, and enzymes [35]. The evaluation of drug likeliness was based on Lipinski's rule of five.

3.4. Biological Activities

3.4.1. Cytotoxicity Assay against HepG2 Human Cell Line

HepG2 human hepatocyte carcinoma cell line was purchased from European Collection of Authenticated Cell Cultures (ECACC). HepG2 cells (ECACCC# 85011430) were cultured in Dulbecco's Modified Eagle's Medium (DMEM) supplemented with 10% fetal bovine serum, antibiotic-antimycotic (100 U/mL penicillin-streptomycin and 0.25 µg amphotericin B) and 2 mM L-glutamine at 37 °C in an atmosphere containing 5% CO₂. The 3-(4,5-dimethylthiazol-2-yl)-2,5-diphenyltetrazolium bromide (MTT) method, described in Gaspar et al., [50] was used for assaying cell viability. Briefly, the cells were grown in the supplemented medium in 96-well microplates in an incubator with 5% CO₂ at 37 °C, until reaching 100% confluence. After growth, the medium was replaced by the compounds' solutions at different concentrations. The compounds were solubilized in supplemented medium containing 0.5% DMSO final concentration. Cells treated only with medium containing 0.5% DMSO served as a negative control. After 24 h incubation, the compound's solutions were replaced by 100 µL of 0.5 mg/mL MTT solution in DMEM culture medium and incubated at 37 °C, 5% CO₂ for 2–4 h. The formed formazan crystals were dissolved in 200 µL of methanol and the absorbance at 595 nm was registered against 630 nm (reference wavelength). For each concentration of the compounds, the percentage of growth inhibition/cytotoxicity was evaluated considering 100% of viability for the absorbance of the negative control. Dose-response curves for each compound were plotted using the Graph Pa Prim 4.0 software and the effective concentration leading to the death of 50% of the cells (EC₅₀) was calculated. All experiments were replicated at least six times.

3.4.2. AChE Inhibition Assay

The inhibition of acetylcholinesterase (AChE) enzymatic activity was measured using the Ellman's colorimetric method with some alterations [51]. Briefly, 325 µL of 50 mM Tris-HCl buffer (pH 8), 100 µL of a compound's solution with 1% DMSO, and 25 µL of AChE (0.1 U/mL) in 50 mM Tris-HCl buffer pH 8 were incubated for 15 min. Subsequently, 75 µL of acetylthiocholine iodide (AChI) (0.023 mg/mL) and 475 µL of 3 mM

5,5'-dithiobis(2-nitrobenzoic acid) (DTNB) in Tris-HCl buffer (pH 8) containing 0.05 M NaCl and 0.021 M MgCl₂ were added to initiate the reaction. The initial rate of the enzymatic reaction was quantified by measuring the absorbance at 405 nm for 5 min (V[compound]). A control reaction was carried out using 1% DMSO water solution, instead of the compound's solution, and this initial rate was considered 100% of the enzymatic activity, V_{control}. The percentage of AChE inhibition (I) for various concentrations of the different compounds was determined as the ratio of V[compound] and V_{control}. For each compound, both the AChEIC₅₀ value (the concentration that inhibits 50% of the AChE activity) and the percentage of inhibition at the compound concentration of 50 μM (Inhibition_{50μM}) were calculated by plotting I for each compound concentration. All the assays were carried out in triplicate.

3.4.3. Molecular Docking

Molecular docking was performed using AutoDock Vina v.1.2.0 software, CCSSB. Both the compounds and the enzyme (PDB ID: 4EY7) were prepared for docking simulations via DockPrep. This function of Chimera 1.16 software removed water molecules and added hydrogens to the compounds, which structure was obtained through ChemDraw software. Five models were generated for each compound, and the highest-scoring model was viewed and analyzed using the Discovery Studio software (BIOVIA, San Diego, CA, USA).

4. Conclusions

A microwave-assisted protocol was successfully established for the synthesis of 2-substituted-1,4-NQ and 4-substituted-1,2-NQ derivatives, with good yields and completing the reactions in shorter times. The electrochemical properties showed to be driven by the reductive processes within the NQ moiety, and the 1,2-NQ series showed to be easier reduced than the corresponding 1,4-NQ series. Moreover, the trend in the redox potential within each series is clearly related to the electronic properties of the amine substituents.

The potential biological activity of the compounds was assessed for their cytotoxicity against HepG2 cell lines and as AChE inhibitors, showing that 1,2-NQ series exhibit a dual action, both as promising cytotoxic agents and moderate AChE inhibitors. The results showed a dependence on chemical modifications in the NQ moiety with an increase in cytotoxic and AChE inhibitory effects, in particular, for electron-donating substituted aromatic amines. Comparison between biological activities and electrochemical parameters showed that the first wave reduction potential is an important parameter as follows: the most easily reduced naphthoquinones ($>E_{pc}$) were the most active against the HepG2 cancer cell lines and as AChE inhibitors. The observed trend suggests that the bioreduction may play an important role in the biological activity of these compounds, but other factors must also be considered.

To elucidate the possible mechanism of AChE targeting action, docking simulations were performed for the more active compounds (**4b** and **4h**), confirming that both compounds interact with amino acid residues in the PAS and CAS of the AChE active site through hydrogen binding and hydrophobic interactions. These interactions, also found for dual-binding cholinesterase inhibitors, such as donepezil, may be related to the good inhibition profiles found for the 4-substituted-1,2-NQ family.

Supplementary Materials: The following supporting information can be downloaded at: <https://www.mdpi.com/article/10.3390/molecules28031232/s1>, Figure S1, HPLC profiles of (A) 1,4-NQ; (B) 1,4-PDA and (C) MA synthesis of **3a**, at optimized conditions (entry 15–Table 1); Figures S2–S14, Cyclic voltammograms of the compounds in ACN + TBAPF₆; Figures S15 and S16, Cytotoxicity profiles in HepG2 human cell line. Figures S17–S49, NMR data in MeOD-*d*₄ (400MHz); Figures S50–S58, ESI/MS spectra; Figures S59–S66, HR ESI/MS spectra; Tables S1 and S2, Electrochemical parameters in acetonitrile (scan rate: 0.100 V·s⁻¹); Tables S3 and S4, Lipinski's parameters estimated using Molinspiration; Table S5, Bioactivity scores of compounds **1**, **2**, **3a–f**, and **4a–h** estimated using Molinspiration; Table S6, The EC₅₀ values for the cytotoxicity of compounds **1**, **2**, **3a–f**, and **4a–h** and reference inhibitor doxorubicin against HepG2 cell line; Table S7, AChE Inhibition_{50μM}

values for compounds **1**, **2**, **3a–f**, and **4a–h**; Tables S8–S10, Molecular docking results of **3b**, **4b**, and **4h**, respectively.

Author Contributions: Conceptualization, A.C.S. and M.P.R.; methodology, R.G.C., G.V., R.P., A.C.S. and M.P.R.; software G.V.; validation, R.G.C., G.V., R.P., A.C.S. and M.P.R.; formal analysis, R.G.C., G.V., R.P., A.C.S. and M.P.R.; investigation, R.G.C., G.V., A.C.S. and M.P.R.; writing—original draft preparation, R.G.C., G.V. and A.C.S.; writing—review and editing, A.C.S., R.P. and M.P.R.; visualization, A.C.S., R.P. and M.P.R.; supervision, A.C.S. and M.P.R.; project administration, A.C.S.; funding acquisition, A.C.S. and M.P.R. All authors have read and agreed to the published version of the manuscript.

Funding: This research was funded by the Instituto Politécnico de Lisboa, project IPL/2021/Naf4Med 3D_ISEL and Fundação para a Ciência e Tecnologia (FCT), Portugal: projects UIDB/00100/2020, UIDP/00100/2020 and Institute of Molecular Sciences (IMS) Associate Laboratory (project LA/P/0056/2020).

Institutional Review Board Statement: Not applicable.

Informed Consent Statement: Not applicable.

Data Availability Statement: Not applicable.

Acknowledgments: Authors gratefully acknowledge IST NMR and MS Networks for facilities and the HPLC analysis performed by Eng. João Costa at PharmaLAB funded by 9^oW program of Hovione SA.

Conflicts of Interest: The authors declare no conflict of interest.

References

1. Han-Yue, Q.; Peng-Fei, W.; Hong-Yan, L.; Cheg-Yi, T.; Hai-Liang, Z.; Yong-Hua, Y. Naphthoquinones: A continuing source for discovery of therapeutic antineoplastic agents. *Chem. Biol. Drug Des.* **2018**, *91*, 681–690.
2. Fiorito, S.; Genovese, S.; Taddeo, V.A.; Mathieu, V.; Kiss, R.; Epifano, F. Novel juglone and plumbagin 5-O derivatives and their in vitro growth inhibitory activity against apoptosis-resistant cancer cells. *Bioorg. Med. Chem. Lett.* **2016**, *26*, 334–337. [[CrossRef](#)] [[PubMed](#)]
3. López, J.; de la Cruz, F.; Alcaraz, Y.; Delgado, F.; Vázquez, M.A. Quinoid systems in chemistry and pharmacology. *Med. Chem. Res.* **2015**, *24*, 3599–3620. [[CrossRef](#)]
4. Louvis, A.R.; Silva, N.A.A.; Semaan, F.S.; da Silva, F.C.; Saramago, G.; de Souza, L.C.S.V.; Ferreira, B.L.A.; Castro, H.C.; Salles, J.P.; Souza, A.L.A.; et al. Synthesis, characterization and biological activities of 3-aryl-1,4-naphthoquinones—Green palladium-catalysed Suzuki cross coupling. *New J. Chem.* **2016**, *40*, 7643–7656. [[CrossRef](#)]
5. Aminin, D.; Polonik, S. 1,4-Naphthoquinones: Some Biological Properties and Application. *Chem. Pharm. Bull.* **2020**, *68*, 46–57. [[CrossRef](#)] [[PubMed](#)]
6. Silva, T.L.; de Azevedo, M.L.S.G.; Ferreira, F.R.; Santos, D.C.; Amatore, C.; Goulart, M.O.F. Quinone-based molecular electrochemistry and their contributions to medicinal chemistry: A look at the present and future. *Curr. Opin. Electrochem.* **2020**, *24*, 79–87. [[CrossRef](#)]
7. da Paiva, T.G.; Silva, T.L.; Xavier, A.F.A.; Cardoso, M.F.C.; da Silva, F.C.; Silva, M.F.S.; Pinheiro, D.P.; Pessoa, C.; Ferreira, V.F.; Goulart, M.O.F. Relationship between Electrochemical Parameters, Cytotoxicity Data against Cancer Cells of 3-Thio-Substituted Nor-Beta-Lapachone Derivatives. Implications for Cancer Therapy. *J. Braz. Chem. Soc.* **2019**, *30*, 658–672. [[CrossRef](#)]
8. Masek, A.; Chrzescijanska, E.; Latos-Brozio, M.; Zaborski, M. Characteristics of juglone (5-hydroxy-1,4-naphthoquinone) using voltammetry and spectrophotometric methods. *Food Chem.* **2019**, *301*, 125279–125286. [[CrossRef](#)]
9. Janeczko, M.; Demchuk, O.M.; Strzelecka, D.; Kubiński, K.; Masłyk, M. New family of antimicrobial agents derived from 1,4-naphthoquinone. *Eur. J. Med. Chem.* **2016**, *124*, 1019–1025. [[CrossRef](#)] [[PubMed](#)]
10. Gonçalves, J.C.R.; Couliadiati, T.H.; Monteiro, A.L.; de Carvalho-Gonçalves, L.C.T.; Valença, W.O.; de Oliveira, R.N.; Câmara, C.A.; de Araújo, D.A.M. Antitumoral activity of novel 1,4-naphthoquinone derivative involves L-type calcium channel activation in human colorectal cancer cell line. *J. Appl. Biomed.* **2016**, *14*, 229–234. [[CrossRef](#)]
11. Kubanik, M.; Kandioller, W.; Kim, K.; Anderson, R.F.; Klapproth, E.; Jakupec, M.A.; Roller, A.; Söhnle, T.; Keppler, B.K.; Hartinger, C.G. Towards targeting anticancer drugs: Ruthenium(ii)–arene complexes with biologically active naphthoquinone-derived ligand systems. *Dalton Trans.* **2016**, *45*, 13091–13103. [[CrossRef](#)]
12. Cardoso, S.H.; de Oliveira, C.R.; Guimarães, A.S.; Nascimento, J.; Carmo, J.O.S.; Ferro, J.N.S.; Correia, A.C.C.; Barreto, E. Synthesis of newly functionalized 1,4-naphthoquinone derivatives and their effects on wound healing in alloxan-induced diabetic mice. *Chem. Biol. Interact.* **2018**, *291*, 55–64. [[CrossRef](#)] [[PubMed](#)]
13. Wu, L. Synthesis and biological evaluation of novel 1,2-naphthoquinones possessing tetrazolo[1,5-a]pyrimidine scaffolds as potent antitumor agents. *RSC Adv.* **2015**, *5*, 24960–24965. [[CrossRef](#)]

14. Shukla, S.; Srivastava, R.S.; Shrivastava, S.K.; Sodhi, A.; Kumar, P. Synthesis, characterization and antiproliferative activity of 1,2-naphthoquinone and its derivatives. *Appl. Biochem. Biotechnol.* **2012**, *167*, 1430–1445. [[CrossRef](#)]
15. Hartfield, M.J.; Chen, J.; Fratt, E.M.; Chi, L.; Bollinger, J.C.; Binder, R.J.; Bowling, J.; Hyatt, J.L.; Scarborough, J.; Jeffries, C.; et al. Selective Inhibitors of Human Liver Carboxylesterase Based on a β -Lapachone Scaffold: Novel Reagents for Reaction Profiling. *J. Med. Chem.* **2017**, *60*, 1568–1579. [[CrossRef](#)]
16. Shin, N.N.; Jeon, H.; Jung, Y.; Baek, S.; Lee, S.; Yoo, H.C.; Bae, G.H.; Park, K.; Yang, S.H.; Han, J.M.; et al. Fluorescent 1,4-Naphthoquinones To Visualize Diffuse and Dense-Core Amyloid Plaques in APP/PS1 Transgenic Mouse Brains. *ACS Chem. Neurosci.* **2019**, *10*, 3031–3044. [[CrossRef](#)] [[PubMed](#)]
17. Wang, H.; Luo, Y.H.; Shen, G.N.; Piao, X.J.; Xu, W.T.; Zhang, Y.; Wang, H.X.; Wang, C.Y.; Jin, C.H. Two novel 1,4-naphthoquinone derivatives induce human gastric cancer cell apoptosis and cell cycle arrest by regulating reactive oxygen species-mediated MAPK/Akt/STAT3 signaling pathways. *Mol. Med. Rep.* **2019**, *20*, 2571–2582. [[CrossRef](#)]
18. Campora, M.; Francesconi, V.; Schenone, S.; Tasso, B.; Tonelli, M. Journey on Naphthoquinone and Anthraquinone Derivatives: New Insights in Alzheimer's Disease. *Pharmaceuticals* **2021**, *14*, 33. [[CrossRef](#)] [[PubMed](#)]
19. Boonyaketguson, S.; Rukachaisirikul, V.; Phongpaichit, S.; Trisuwa, K. Naphthoquinones from the leaves of *Rhinacanthus nasutus* having acetylcholinesterase inhibitory and cytotoxic activities. *Fitoterapia* **2018**, *124*, 206–210. [[CrossRef](#)] [[PubMed](#)]
20. Ahmadi, E.S.; Tajbakhsh, A.; Iranshahy, M.; Asili, J.; Kretschmer, N.; Shakeri, A.; Sahebkar, A. Naphthoquinone Derivatives Isolated from Plants: Recent Advances in Biological Activity. *Mini-Rev. Med. Chem.* **2020**, *20*, 2019–2035. [[CrossRef](#)] [[PubMed](#)]
21. Estolano-Cobián, A.; Noriega-Iribe, E.; Díaz-Rubio, L.; Padrón, J.M.; Brito-Perea, M.; Cornejo-Bravo, J.M.; Chávez, D.; Rivera, R.R.; Quintana-Melgoza, J.M.; Cruz-Reyes, J.; et al. Antioxidant, antiproliferative, and acetylcholinesterase inhibition activity of amino alcohol derivatives from 1,4-naphthoquinone. *Med. Chem. Res.* **2020**, *29*, 1986–1999. [[CrossRef](#)]
22. Nepovimosa, E.; Uliassi, E.; Korabecny, J.; Peña-Altamira, L.E.; Samez, S.; Pesaresi, A.; Garcia, G.E.; Bartolini, M.; Andrisano, V.; Bergamini, C.; et al. Multitarget Drug Design Strategy: Quinone–Tacrine Hybrids Designed To Block Amyloid- β Aggregation and To Exert Anticholinesterase and Antioxidant Effects. *J. Med. Chem.* **2014**, *57*, 8576–8589. [[CrossRef](#)]
23. Johnson, G.; Moore, S.W. The peripheral anionic site of acetylcholinesterase: Structure, functions and potential role in rational drug design. *Curr. Pharm. Des.* **2006**, *12*, 217–225. [[CrossRef](#)] [[PubMed](#)]
24. Hansen, R.A.; Gartlehner, G.; Webb, A.P.; Morgan, L.C.; Moore, D.E.J. Efficacy and safety of donepezil, galantamine, and rivastigmine for the treatment of Alzheimer's disease: A systematic review and meta-analysis. *Clin. Interv. Aging* **2008**, *3*, 211–225. [[PubMed](#)]
25. Jordão, A.K.; Novais, J.; Leal, B.; Escobar, A.C.; Santos Jr, H.M.; Castro, H.C.; Ferreira, V.F. Synthesis using microwave irradiation and antibacterial evaluation of new N,O-acetals and N,S-acetals derived from 2-amino-1,4-naphthoquinones. *Eur. J. Med. Chem.* **2013**, *63*, 196–201. [[CrossRef](#)]
26. Kittakoop, P.; Mahidol, C.; Ruchirawat, S. Alkaloids as important scaffolds in therapeutic drugs for the treatments of cancer, tuberculosis, and smoking cessation. *Curr. Top. Med. Chem.* **2014**, *14*, 239–252. [[CrossRef](#)] [[PubMed](#)]
27. Liu, Y.; Ge, H. Site-selective C–H arylation of primary aliphatic amines enabled by a catalytic transient directing group. *Nat. Chem.* **2016**, *9*, 26–32. [[CrossRef](#)]
28. Leyva, E.; Cárdenas-Chaparro, A.; Loredó-Carrillo, S.E.; López, L.I.; Méndez-Sánchez, F.; Martínez-Richa, A. Ultrasound-assisted reaction of 1,4-naphthoquinone with anilines through an EDA complex. *Mol. Divers.* **2018**, *22*, 281–290. [[CrossRef](#)]
29. López-López, L.I.; Garcia, J.J.V.; Sáenz-Galindo, A.; Silva-Belmares, S.Y. Ultrasonic and Microwave Assisted Synthesis of Nitrogen-Containing Derivatives of Juglone as Potential Antibacterial Agents. *Lett. Org. Chem.* **2014**, *11*, 573–582. [[CrossRef](#)]
30. Berrino, E.; Supuran, C.T. Advances in microwave-assisted synthesis and the impact of novel drug discovery. *Expert Opin. Drug Discov.* **2018**, *13*, 861–873. [[CrossRef](#)]
31. Rath, A.K.; Gawande, M.B.; Zboril, R.; Varma, R.S. Microwave-assisted synthesis—Catalytic applications in aqueous media. *Coord. Chem. Rev.* **2015**, *291*, 68–94. [[CrossRef](#)]
32. Sousa, A.C.; Santos, I.; Piedade, M.F.M.M.; Martins, L.O.; Robalo, M.P. Synthesis of Substituted 4-Arylamino-1,2-naphthoquinones in One-Pot Reactions Using CotA-Laccase as Biocatalyst. *Adv. Synth. Catal.* **2020**, *362*, 3380–3387. [[CrossRef](#)]
33. Amatore, C.; Labbé, E.; Buriez, O. Molecular electrochemistry: A central method to understand the metabolic activation of therapeutic agents. The example of metalocifen anti-cancer drug candidates. *Curr. Opin. Electrochem.* **2017**, *2*, 7–12. [[CrossRef](#)]
34. De Abreu, F.C.; Ferraz, P.A.L.; Coulart, M.O.F.; Some Applications of Electrochemistry in Biomedical Chemistry. Emphasis on the Correlation of Electrochemical and Bioactive Properties. *J. Braz. Chem. Soc.* **2002**, *13*, 19–35. [[CrossRef](#)]
35. Kovacic, P.; Becvar, L.E. Mode of action of anti-infective agents: Focus on oxidative stress and electron transfer. *Curr. Pharm. Des.* **2000**, *6*, 143–167. [[CrossRef](#)] [[PubMed](#)]
36. Molinspiration Cheminformatics. Available online: molinspiration.com (accessed on 5 July 2022).
37. Lipinski, C.A.; Lombardo, F.; Dominy, B.W.; Feeney, P. Experimental and computational approaches to estimate solubility and permeability in drug discovery and development settings. *Adv. Drug Deliv. Rev.* **2001**, *46*, 3–26. [[CrossRef](#)] [[PubMed](#)]
38. Zhao, Y.H.; Abraham, M.H.; Le, J.; Hersey, A.; Luscombe, C.N.; Beck, G.; Sherborne, B.; Cooper, I. Rate-limited steps of human oral absorption and QSAR studies. *Pharm. Res.* **2002**, *19*, 1446–1457. [[CrossRef](#)]
39. Mahmoud, I.S.; Hatmal, M.M.; Abuarqoub, D.; Esawi, E.; Zalloum, H.; Wehaibi, S.; Nsairat, H.; Alshaer, W. 1,4-Naphthoquinone is a Potent Inhibitor of IRAK1 Kinases and the Production of Inflammatory Cytokines in THP-1 Differentiated Macrophages. *ACS Omega* **2021**, *6*, 25299–25310. [[CrossRef](#)]

40. Brien, Z.O.; Moghaddam, M.F. A systematic analysis of physicochemical and ADME properties of all small molecule kinase inhibitors approved by US FDA from January 2001 to October 2015. *Curr. Med. Chem.* **2017**, *24*, 3159–3184.
41. Arzumian, V.A.; Kiseleva, O.I.; Poverennaya, E.V. The curious case of HepG2 cell line: 40 years of expertise. *Int. J. Mol. Sci.* **2021**, *22*, 13135. [[CrossRef](#)]
42. Copeland, R.A.; Harpel, M.R.; Tummino, P.J. Targeting enzyme inhibitors in drug discovery. *Expert Opin. Ther. Targets* **2007**, *11*, 967–978. [[CrossRef](#)] [[PubMed](#)]
43. Mosmann, T. Rapid colorimetric assay for cellular growth and survival: Application to proliferation and cytotoxicity assays. *J. Immunol. Methods* **1983**, *65*, 55–63. [[CrossRef](#)]
44. Jacobs, N.; Lang, S.; Panisch, R.; Wittstock, G.; Growth, U.; Nasiri, H.R. Investigation on the electrochemistry and cytotoxicity of the natural product marcanine A and its synthetic derivatives. *RSC Adv.* **2015**, *5*, 58561–58565. [[CrossRef](#)]
45. Powis, G. Free radical formation by antitumor quinones. *Free Radic. Biol. Med.* **1989**, *6*, 63–101. [[CrossRef](#)]
46. Bai, D.L.; Tang, X.C.; He, X.C. Huperzine A, a potential therapeutic agent for treatment of Alzheimer's disease. *Curr. Med. Chem.* **2000**, *7*, 355–374. [[CrossRef](#)]
47. Cheung, J.; Rudolph, M.J.; Burshteyn, F.; Cassidy, M.S.; Gary, E.N.; Love, J.; Franklin, M.C.; Height, J.J. Structures of Human acetylcholinesterase in complex with pharmacologically important ligands. *J. Med. Chem.* **2012**, *55*, 10282–10286. [[CrossRef](#)] [[PubMed](#)]
48. Li, Q.; He, S.; Chen, Y.; Feng, F.; Qu, W.; Sun, H. Donepezil based multi-functional cholinesterase inhibitors for treatment of Alzheimer's disease. *Eur. J. Med. Chem.* **2018**, *158*, 463–477. [[CrossRef](#)] [[PubMed](#)]
49. Alipour, M.; Khoobi, M.; Foroumadi, A.; Nadri, H.; Moradi, A.; Sakhteman, A.; Ghandi, M.; Shafiee, A. Novel coumarin derivatives bearing N-benzyl pyridinium moiety: Potent and dual binding site acetylcholinesterase inhibitors. *Bioorg. Med. Chem.* **2012**, *20*, 7214–7222. [[CrossRef](#)]
50. Gaspar, H.; Bronze, S.; Oliveira, C.; Victor, B.L.; Machuqueiro, M.; Pacheco, R.; Caldeira, M.J.; Santos, S. Proactive Response to Tackle the Threat of Emerging Drugs: Synthesis and Toxicity Evaluation of New Cathinones. *Forensic Sci. Int.* **2018**, *290*, 146–156. [[CrossRef](#)]
51. Silva, A.F.C.; Haris, P.I.; Serralheiro, M.L.; Pacheco, R. Mechanism of action and the biological activities of *Nigella sativa* oil components. *Food Biosci.* **2020**, *38*, 100783. [[CrossRef](#)]

Disclaimer/Publisher's Note: The statements, opinions and data contained in all publications are solely those of the individual author(s) and contributor(s) and not of MDPI and/or the editor(s). MDPI and/or the editor(s) disclaim responsibility for any injury to people or property resulting from any ideas, methods, instructions or products referred to in the content.